Electron-momentum distributions in singly ionizing C^{6+}-He collisions at intermediate velocities

M. A. Abdallah,* C. L. Cocke,† W. Wolff,‡ H. E. Wolf,‡ and M. Stöckli
Physics Department, J. R. Macdonald Laboratory, Kansas State University, Manhattan, Kansas 66506-2601
(Received 11 August 2000; published 16 January 2001)

The process of single ionization has been studied in C^{6+}-He collisions at the collision velocities of 1.17, 1.36, and 1.63 a.u. Ejected electrons were detected in coincidence with the recoil ions. Two components of the electron-momentum and the full-momentum vector of the recoil ion were measured. From these, two-dimensional momentum-space distributions of the continuum electrons were deduced, projected parallel or perpendicular to the collision plane, and for several values of the recoil transverse momentum. The distributions do not show the molecular-orbital-like patterns seen in similar collisions with singly and doubly charged projectiles. They do tend to lie preferentially along a ridge joining the target and projectile velocities, and show an increasing tendency to go in the direction of the projectile, both longitudinally and transversely, as the collision velocity is raised and the impact parameter lowered. The results are in agreement with classical trajectory Monte Carlo predictions for similar systems.

DOI: 10.1103/PhysRevA.63.024702 PACS number(s): 34.50.Fa

When a highly charged ion collides with an atom, one or more of the target atom electrons can be liberated to the continuum in a process known as ionization. The analysis of the energy and momentum of the ionized electron is a primary tool for studying the ionization mechanisms [1]. While ionization mechanisms are well understood at large collision velocities ($v_p \gg v_0$, where v_p and v_0 are projectile velocity and target classical bound electron velocity, respectively), they have remained a subject of debate at low velocities ($v_p \lesssim v_0$). At intermediate to high velocities, two major mechanisms that have been identified as giving rise to continuum electrons are soft-electron emission (SEE) and electron capture to the continuum (ECC). In momentum space, electrons produced through these two processes are centered on the target and on the projectile velocities (multiplied by the electron mass), respectively. At low projectile velocities, a third mechanism (saddle-point mechanism) was suggested [2,3] that would produce electrons centered on the equiforce point (saddle point) between the target and the projectile. This suggestion was followed by a great deal of controversy, and experiments were reported that both support, and do not support, the importance of such a mechanism [4].

We have previously reported emitted electron momentum distributions (EEMDs) for different collision systems obtained using imaging techniques and position sensitive detectors [5–7]. Unlike conventional electron spectroscopy, which measures electron energy at a certain ejection angle, the imaging method measures two-dimensional soft electron momentum distributions in one ''snapshotlike'' image. Using this technique, we found that the EEMDs strongly depend on the charge and velocity of the projectile ion, and also on the target atom. In general, we found that the emitted electrons are strongly focused in the forward direction in the laboratory frame. The EEMD peak position in the longitudinal direction was found to shift toward the projectile velocity with an increasing projectile charge state, opposite to what was expected from simple saddle-point arguments. For C^{6+}, O^{8+}, and Ne^{10+} colliding with He and Ne, we found that the EEMD peak in the longitudinal direction was centered nearly on the projectile velocity. The results of these experiments were in fair agreement with continuum-distorted-wave-eikonal-initial-state calculations (CDW-EIS) [5–9], but in not as good agreement with classical trajectory Monte Carlo (CTMC) calculations [5,10].

With the development of cold-target recoil-ion momentum spectroscopy (COLTRIMS) [11,12], it has become possible to study this process with more complete experimental control over the collision parameters. By detecting electrons in coincidence with fully momentum-analyzed recoil ions, one obtains not only the EEMDs, but the dependence of these distributions on the transverse and longitudinal momentum transferred to the recoil in the collision. The transverse recoil momentum determines the collision plane and can be used to determine quantitatively the impact parameter for the collision if a suitable effective heavy-ion scattering potential is known. The longitudinal recoil momentum measures the inelasticity of the collision. Using this technique, previous studies of ionization in collisions of p, He^+, He^{2+}, and Ne^+ with He, Ne, and H_2 [13–18] have been carried out. These highly differential experiments revealed striking patterns in the EEMDs, which were interpreted as reflecting the structure of the molecular orbitals whose promotion into the continuum was responsible for the ionization. These collision systems all involved singly or doubly charged projectiles, for which the main population in the EEMDs centers in the vicinity of the saddle point longitudinally. As the projectile charge is raised, one would expect the molecular structures to become less well defined, as the promotion paths become less obvious. Furthermore, the evolution of the EEMDs away from the saddle region toward the projectile suggests that a different picture of the process might be necessary. The main purpose of this investigation is to use the full experimental control over the collision plane and transverse heavy particle momentum transfer to examine how the mo-

*Present address: KLA-Tencor Corp., San Jose, CA 95134. Email address: mohammad.abdallah@kla-tencor.com
†Email address: cocke@phys.ksu.edu
‡Permanent address: Instituto de Fisica, Universidade Federal do Rio de Janeiro, Rio de Janeiro, Brazil.

lecular structures seen for singly and doubly charged systems evolve as the projectile charge is raised.

We have investigated single ionization in C^{6+}-He collisions at projectile velocities $v_p = 1.17$, 1.36, and 1.63 a.u. We used the same technique of combined electron and recoil-ion detection used in earlier COLTRIMS experiments [14–18]. A detailed description of the experimental setup and data analysis can be found elsewhere [14]. Briefly, the ion beam (z direction) intersects with a target supersonic He gas jet (y direction) at 90°. An electric field perpendicular to the ion beam and the gas jet (x direction) is used to extract the recoil ions and electrons from the collision area in opposite directions. The recoil ions and electrons are detected by two two-dimensional position sensitive detectors (2DPSDs) placed on the opposite ends of the extraction region (in the yz plane). The electron position (z,y) on the electron 2DPSD was used to reconstruct two components (v_{ez}, v_{ey}) of its initial velocity (momentum). The recoil-ion position and its time of flight were used to reconstruct its full momentum vector, where the timing start signal was taken from the corresponding electron signal. Two-dimensional (v_{ez}, v_{ey}) EEMDs were produced for different conditions on the direction of emission of the recoil ions. Two particular EEMDs are of interest: (1) one for which the recoil-ion momenta are required to lie parallel to the plane of the electron detector, which yields a ''top view'' of the emitted electrons, looking down on the collision plane, and (2) one for which the recoil momenta are required to lie perpendicular to the plane of the electron detector, which yields a ''side view'' of the ejected electrons, looking edge-on along the collision plane. For each of the above views, further selection of small or large impact parameter collisions was made by selecting the magnitude of the transverse recoil momentum vector.

In Fig. 1 we show the EEMDs for single ionization in C^{6+}-He collisions at $v_p = 1.63$ a.u. All electron spectra are integrated over the third velocity component v_{ex}, which has not been measured in this experiment. Dashed and solid lines guide the eye to the target and projectile laboratory-frame velocities, respectively. Seven contour lines are used to present the intensity in every plot on a linear scale. Figure 1(a) shows the top view of the emitted electrons. In this figure, recoil ions are emitted downward (negative y direction). Figure 1(b) shows a side view of the emitted electrons where the recoil ions are emitted into the page (x direction). Figure 1(c) shows the electron momentum distribution with no specific direction of recoil-ion transverse momentum selected. These spectra are gated on recoil ions with transverse momentum $p_{r\perp} \leqslant 1.8$ a.u., which covers the major part of the cross section. It is noted that most of the emitted electrons form a narrow ridge between the target and projectile velocities, in agreement with previous observations [5–7,10]. As one expects, the distributions in (b) and (c) are symmetric in the transverse direction. However, the symmetry is broken in (a). Electrons are preferentially emitted away from the recoil ions and in the direction of deflection of the projectiles. This asymmetry increases with emitted electron energy and maximizes near the projectile velocity v_p. Although asymmetry in electron transverse velocity has been observed in other systems [13–18], the shape of the distribution for

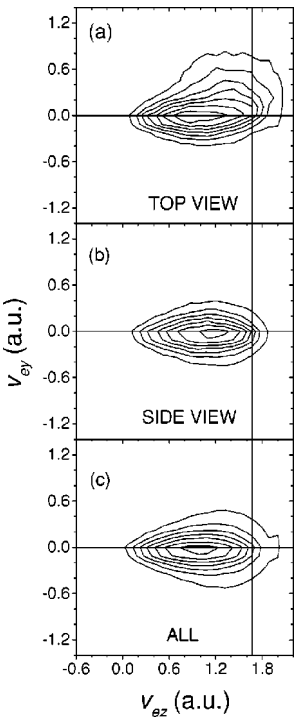

FIG. 1. Emitted electron momentum distributions in singly ionizing C^{6+}-He collisions at collision velocity $v_p = 1.63$ a.u. (a) Electron momentum top view, recoil ions are in the y direction. (b) Electron momentum side view, recoil ions are in the x direction. In (c) no collision plane is selected. In each plot, intensity is represented by seven contours on a linear scale. Dashed and solid lines guide the eye to the laboratory-frame target and projectile velocities, respectively.

this system is different from the shapes of distributions seen in earlier experiments. The marked molecular-orbital-like structure seen for singly and doubly charged systems is no longer present. In particular, the two-branch pattern that has been seen in the collisions of p, He^+, and He^{2+} with He is not present. The side-view distribution [Fig. 1(b)] is slightly narrower than the top-view distribution, indicating that the ejected electrons have a slight preference for staying in the collision plane. This behavior has also been observed in other systems [13–18].

We now address the dependence of these patterns on the transverse momentum transfer to the recoil. This momentum is approximately a measure of the impact parameter, since the transverse momentum transfer to the electrons is small. To show the range of transverse recoil momenta involved, we show in Fig. 2 recoil-ion transverse momentum distributions for the three collision velocities. It is noted that these distributions show no significant change with changing collision velocity. A slight shift in peak position toward larger momentum can be seen with decreasing collision velocity. In Fig. 3 we show how the structure of the EEMDs varies with increasing impact parameter. Each column shows top-view EEMDs for a single collision velocity. The first three rows show how the EEMDs evolve as the transverse recoil momentum $p_\perp$ is increased (i.e., the impact parameter is decreased). Each row is labeled by the range in $p_\perp$ (in a.u.). For a Coulomb encounter, the transverse recoil momentum is

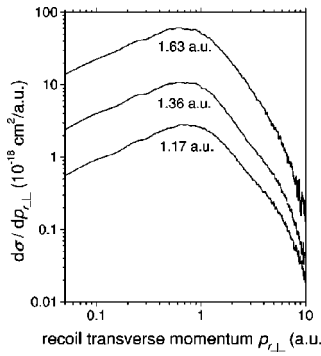

FIG. 2. Recoil-ion transverse momentum distributions in singly ionizing C^{6+}-He collisions at collision velocities $v_p=1.17$, 1.36, and 1.63 a.u.

related to the impact parameter b by $p_\perp=2Z_aZ_b/bv_P$, where Z_a and Z_b are the effective heavy particle charges and atomic units are used. In all of these plots, the recoil ions are selected to have a transverse momentum in the negative y direction. In general, the ejected electrons form a ridge between target and projectile velocity at all velocities. For the softest collisions (first row), the distributions show little awareness of the recoil direction, and tend to maximize about halfway between projectile and target. (We note, however, that the saddle point for this collision system is very near the target in velocity space, so these electrons are not grouping near the saddle.) As the impact parameter becomes smaller, the tendency for the electrons to follow the projectile and to scatter away from the recoil ion and toward the projectile increases. Ultimately for the hardest collisions (smallest impact parameter; third row), many electrons are even thrown forward of the projectile. This effect is most marked at the highest projectile velocity. A similar asymmetry has been seen using CTMC calculations by Olson *et al.* in the collisions of 165 keV/u C^{6+} [10] and 100–500 keV/u Ne^{10+} [19] with He. Olson *et al.* suggested that this asymmetry is due to the effect of the large projectile charge on the ejected electron, as the ejected electron ''follows'' the deflected projectile.

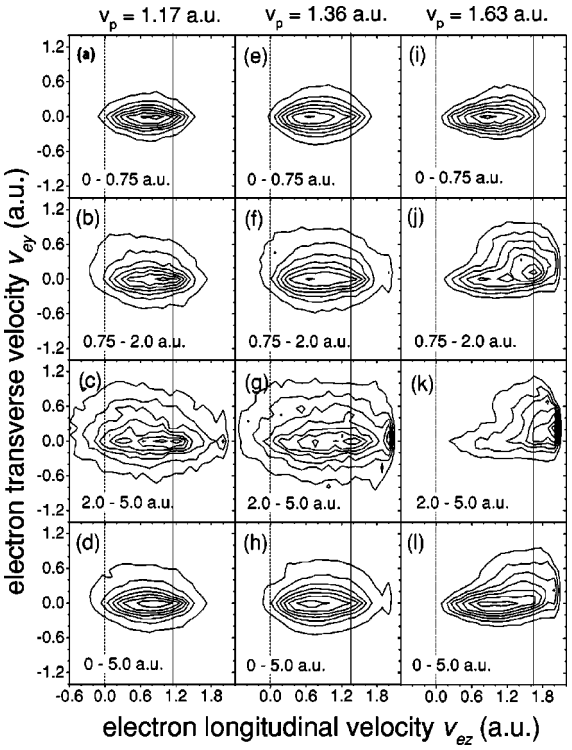

FIG. 3. Top views of the emitted electron momentum distributions for three collision velocities 1.17, 1.36, and 1.63 a.u. Recoil ions are emitted in the y direction. For every velocity, the distribution is gated on three ranges of recoil transverse momentum (0–0.75,0.75–2.0,2.0–5.0 a.u.). Top views with all transverse momentum values are shown in the bottom row. In every plot, seven contours represent the intensity on a linear scale. Dashed and solid lines are to guide the eye to target and projectile velocities, respectively. The apparent cutoff and accumulation at $v_{ez}\simeq 2.0$ a.u. in some plots is an artifact caused by the edge of the position-sensitive detector.

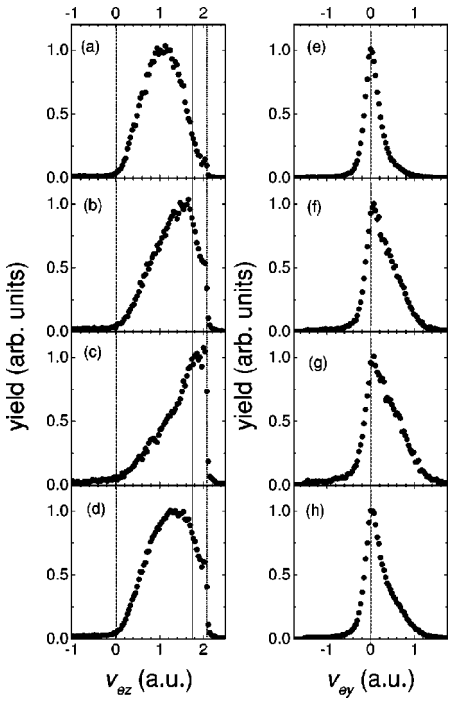

FIG. 4. Corresponding projections of the the distributions in Figs. 3(i)–3(l) on the v_{ez} direction (a)–(d) and on the v_{ey} direction (e)–(h). In (a)–(d), dashed, solid, and dotted lines guide the eye to target velocity, projectile velocity, and detector edge, respectively. In (e)–(h), the dotted line guides the eye to transverse electron momentum $v_{ey}=0$ a.u. All distributions have been normalized to a height of unity.

To study the asymmetry and the peak shift of the top-view EEMDs in the case of $v_p=1.63$ a.u., for which the effects are most marked, we show in Fig. 4 longitudinal (a)–(d) and transverse (e)–(h) projections of the corresponding distributions from Figs. 3(i)–3(l). In Figs. 4(a)–4(c), we see the dramatic shift of electron longitudinal velocity peak position with decreasing impact parameter. The dramatic increase in asymmetry in electron transverse momentum can be seen in Figs. 4(e)–4(g). In general, we notice that the EEMDs have a stronger dependence on impact parameter for $v_p=1.63$ a.u. than for the two lower collision velocities. It is important to

remember that, over this range of collision velocities, electron capture is strongly dominant over ionization as the mechanism of target electron removal. From the results of Wu *et al.* [20], we find that the ratios of single ionization to single capture for $v_p = 1.17$, 1.36, and 1.63 a.u. in C^{6+}-He collisions are 0.004, 0.014, and 0.083, respectively. Therefore, although the collision velocity increases by only 40% in going from the lowest to the highest collision velocity in this experiment, the ratio of single ionization to single capture increases by nearly 20 times. Since capture cross sections at these velocities are nearly independent of collision velocity [21], this rise is due to the fast rise in the single ionization cross section. Based on the two-center atomic orbital close-coupling method, Wang *et al.* [22] explained this strong rise of ionization cross section as being a result of the increasing role of the ECC process with increasing collision velocity relative to the slow rise in the SEE cross section. This suggestion agrees with the present data, since more electrons are produced with velocities near the projectile velocity at higher collision velocities and smaller impact parameters. In general, one can expect an interplay between the SEE process and the ECC process as the major factor determining the shape of the EEMDs. While SEE is relatively more important for large-impact-parameter collisions, ECC seems to be more important at small impact parameters. The dependence on collision velocity is more complex, but in general, at intermediate collision velocities we see a rise in the importance of ECC relative to SEE with increasing collision velocity. Eventually, SEE comes back to be the most important of the two as the process of electron capture itself becomes extremely unlikely compared to direct electron ionization. An interplay of the roles of SEE and ECC processes has been also suggested by Fainstein [23,24] based on the (CDW-EIS) calculations to explain the EEMDs for *p*-He and *p*-Ne collisions at intermediate velocities. However, it is noted that in Fig. 3(k) the distribution in the longitudinal direction does not show the usual symmetry of the ECC process. In fact, the peak position exceeds projectile velocity. No explanation of this behavior is available at this moment.

In conclusion, we have presented emitted electron momentum distributions for C^{6+}-He collisions at intermediate velocities. The results show that most of the emitted electrons form a ridge between the target and projectile in velocity space, which is in agreement with earlier experiments. Top-view distributions show a strong asymmetry in the collision plane, with the electrons being emitted preferentially opposite to the direction of recoil ions. This asymmetry increases with decreasing impact parameter and collision velocity. In the longitudinal direction, the electron momentum distribution peaks at larger velocities with decreasing impact parameter and increasing collision velocity. That is, ECC-like continuum electrons are produced preferentially in small impact parameter collisions. This result is in agreement with CTMC predictions [10,19] for similar collision systems. It appears that the marked molecular-orbital-like structures, which are seen in the EEMDs for lower-charged systems, are lost when the projectile is highly charged as is the case here. In the case of the singly charged systems, which leave two singly charged ions plus one electron in the continuum, it is typically the case that the promotion of a single π or σ molecular orbital dominates the process and the symmetry properties of these orbitals are seen in the EEMDs. This simplicity appears to be lost when the projectile is highly charged. It is known that molecular orbital treatments of electron capture for this system are appropriate and successful [25]. However, many orbitals must be taken into account in order to describe the collision, and thus the simplicity of promoting a single dominant orbital into the continuum seems to be lost. It appears to us that such orbital-specific promotion descriptions for the low-charged systems may have to be replaced by either very complete molecular orbital ones or classical treatments for the highly charged systems.

One of the authors (M.A.A.) gratefully acknowledges the support from the ORNL Postdoctoral Research Associates Program administered jointly by Oak Ridge Institute for Science and Education and Oak Ridge National Laboratory. We gratefully acknowledge numerous helpful discussions with R.E. Olson. This work was supported by the Chemical Sciences, Geosciences and Biosciences Division, Office of Basic Energy Sciences, Office of Science, U.S. Department of Energy.

[1] N. Stolterfoht *et al., Electron Emission in Heavy Ion-Atom Collisions* (Springer Verlag, Berlin, 1997).
[2] R.E. Olson, Phys. Rev. A **27**, 1871 (1983).
[3] T.G. Winter and C.D. Lin, Phys. Rev. A **29**, 3071 (1984).
[4] M. Pieksma, Nucl. Instrum. Methods Phys. Res. B **124**, 177 (1997).
[5] S.D. Kravis *et al.*, Phys. Rev. A **54**, 1394 (1996).
[6] M. Abdallah *et al.*, Phys. Rev. A **56**, 2000 (1997).
[7] M.A. Abdallah *et al.*, Phys. Scr. **T73**, 219 (1997).
[8] Y.D. Wang *et al.*, Phys. Rev. A **53**, 3278 (1996).
[9] V.D. Rodriguez, Nucl. Instrum. Methods Phys. Res. B **132**, 250 (1997).
[10] R.E. Olson *et al.*, Phys. Rev. A **58**, 270 (1998).
[11] J. Ullrich *et al.*, J. Phys. B **30**, 2917 (1997).
[12] R. Dörner *et al.*, Phys. Rep. **330**, 96 (2000).
[13] R. Dörner *et al.*, Phys. Rev. Lett. **77**, 4520 (1996).
[14] M.A. Abdallah *et al.*, Phys. Rev. Lett. **81**, 3627 (1998).
[15] M.A. Abdallah *et al.*, Phys. Rev. A **58**, R3379 (1998).
[16] M.A. Abdallah *et al.*, J. Phys. B **32**, 4237 (1999).
[17] M.A. Abdallah *et al.*, Phys. Scr. **T80**, 405 (1999).
[18] M.A. Abdallah *et al.*, Phys. Rev. A **62**, 012711 (2000).
[19] R.E. Olson *et al.*, Nucl. Instrum. Methods Phys. Res. B **124**, 249 (1997).
[20] W. Wu *et al.*, Phys. Rev. Lett. **75**, 1054 (1995).
[21] W. Wu *et al.*, and M. Stöckli, Phys. Rev. A **50**, 502 (1994).
[22] Y.D. Wang *et al.*, Phys. Rev. A **52**, 2852 (1995).
[23] P.D. Fainstein, J. Phys. B **29**, L763 (1996).
[24] P.D. Fainstein, Phys. Rev. A **60**, R741 (1999).
[25] C. Harel, H. Jouin, and B. Pons, J. Phys. B **29**, L425 (1991).